JB
Journals.ASM.org

Analyses of MbtB, MbtE, and MbtF Suggest Revisions to the Mycobactin Biosynthesis Pathway in *Mycobacterium tuberculosis*

Matthew D. McMahon,[a,b] Jason S. Rush,[c] and Michael G. Thomas[a,b]

Department of Bacteriology, University of Wisconsin—Madison, Madison, Wisconsin, USA[a]; Microbiology Doctoral Training Program, University of Wisconsin—Madison, Madison, Wisconsin, USA[b]; and Department of Molecular, Cellular, and Developmental Biology, Yale University, New Haven, Connecticut, USA[c]

The production of mycobactin (MBT) by *Mycobacterium tuberculosis* is essential for this bacterium to access iron when it is in an infected host. Due to this essential function, there is considerable interest in deciphering the mechanism of MBT assembly, with the goal of targeting select biosynthetic steps for antituberculosis drug development. The proposed scheme for MBT biosynthesis involves assembly of the MBT backbone by a hybrid nonribosomal peptide synthetase (NRPS)/polyketide synthase (PKS) megasynthase followed by the tailoring of this backbone by N^6 acylation of the central L-Lys residue and subsequent N^6-hydroxylation of the central N^6-acyl-L-Lys and the terminal caprolactam. A complete testing of this hypothesis has been hindered by the inability to heterologously produce soluble megasynthase components. Here we show that soluble forms of the NRPS components MbtB, MbtE, and MbtF are obtained when these enzymes are coproduced with MbtH. Using these soluble enzymes we determined the amino acid specificity of each adenylation (A) domain. These results suggest that the proposed tailoring enzymes are actually involved in precursor biosynthesis since the A domains of MbtE and MbtF are specific for N^6-acyl-N^6-hydroxy-L-Lys and N^6-hydroxy-L-Lys, respectively. Furthermore, the preference of the A domain of MbtB for L-Thr over L-Ser suggests that the megasynthase produces MBT derivatives with β-methyl oxazoline rings. Since the most prominent form of MBT produced by *M. tuberculosis* lacks this β-methyl group, a mechanism for demethylation remains to be discovered. These results suggest revisions to the MBT biosynthesis pathway while also identifying new targets for antituberculosis drug development.

The bacterium *Mycobacterium tuberculosis*, the primary causative agent of tuberculosis (TB), infects one-third of the world's population and was responsible for 1.4 million deaths in 2010 (46). A significant challenge in treating *M. tuberculosis* infections is the evolution of strains that are resistant to first- and second-line drugs that are key components of TB treatment (37). To meet this challenge, new anti-TB drugs and new *M. tuberculosis* drug targets must be identified.

One new target for antitubercular drug development is the biosynthesis of mycobactin (MBT) siderophores in *M. tuberculosis*. These iron-chelating molecules are attractive drug targets because *M. tuberculosis* must survive in the phagosomes of macrophages, where it competes with the host for iron (4). Strains of *M. tuberculosis* that are unable to biosynthesize MBTs or import MBTs with chelated iron are impaired in their ability to grow in the lung or macrophages (35), demonstrating the importance of these molecules in causing disease. Furthermore, the addition of small molecules that disrupt MBT biosynthesis inhibited *M. tuberculosis* growth in iron-limiting media (10). These data provide strong support for targeting MBT biosynthesis for drug development.

The MBT siderophores are a family of nonribosomal peptide/polyketide hybrid natural products produced by many mycobacterial species and other actinomycetes (13, 30, 39). *M. tuberculosis* produces both membrane-associated and soluble forms of MBT that have structural differences at two locations (Fig. 1). The most significant structural difference is the variability of acyl group attached to the N^6 of the central L-Lys residue. The membrane-associated MBTs have a long fatty acyl chain, which is capped by a methyl group, while the soluble forms of MBT contain a shorter fatty acyl chain, which is capped with either a carboxylate or methyl ester. The fatty acids may also contain desaturation between the α and β carbons. The second region of structural variation is at the β-carbon of the oxazoline ring. This carbon is unmethylated in the predominant MBT produced by *M. tuberculosis*, MBT T (38), and methylated in a fraction of the soluble MBTs (13). Recent work identified further structural variants of MBT that lack the hydroxyl groups on the N^6 of both L-Lys residues (23, 27); thus they are deficient for two moieties that are needed for iron chelation. These molecules were not identified for their iron-chelating proficiency; rather, they were identified as molecules present in the cell wall of *M. tuberculosis* that stimulate T cell activation (27) or were detected using mass spectrometry (23). These findings were used to suggest that the N^6-hydroxylations are the final steps in MBT biosynthesis. Interestingly, the nonhydroxylated structural variants that stimulated T cell activation contain oxazoline rings that are α-methylated, in contrast to MBT T. MBTs containing α-methylated oxazoline rings have also been identified from *Nocardia* sp. A32030 (43); thus, this form of MBT is also biosynthesized by other actinomycetes, suggesting that *M. tuberculosis* may also form α-methylated MBT derivatives.

The vital role of MBTs in *M. tuberculosis* physiology and virulence has drawn considerable interest in identifying the genes involved in MBT biosynthesis. Initial genome analysis identified a

Received 18 January 2012 **Accepted** 14 March 2012
Published ahead of print 23 March 2012
Address correspondence to Michael G. Thomas, thomas@bact.wisc.edu.
Supplemental material for this article may be found at http://jb.asm.org/.

doi:10.1128/JB.00088-12

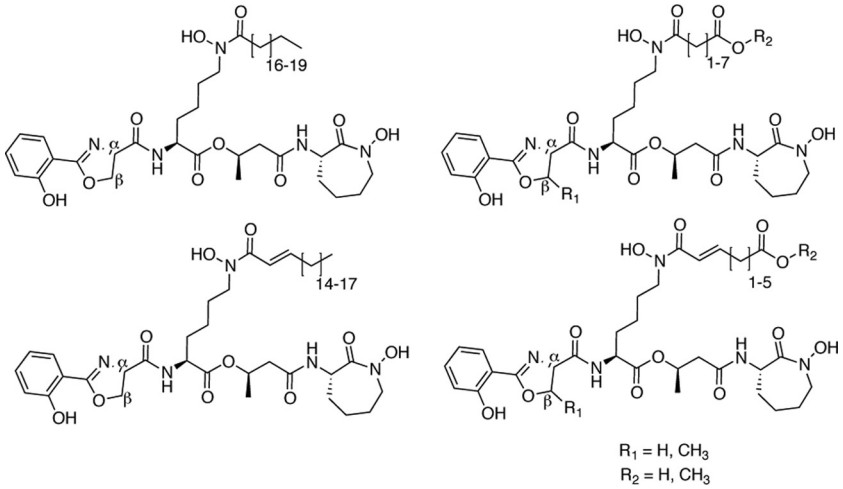

FIG 1 Chemical structures of the MBTs produced by *M. tuberculosis*. The membrane-associated MBTs are on the left; the soluble MBTs are on the right. The α and β designations denote the carbons of the oxazoline ring that may contain a methyl group.

gene cluster (*mbt-1*) in *M. tuberculosis* that codes for salicylate biosynthesis (MbtI), N^6-hydroxylation of L-Lys (MbtG), the hybrid nonribosomal peptide synthetase (NRPS) and polyketide synthase (PKS) megasynthase that assembles MBT (MbtA to -F), and two proteins of unknown function (MbtJ and MbtH) (29). Subsequent genetic studies confirmed that this gene cluster was associated with MBT production in *M. tuberculosis* (4). Analyses of the homologous clusters from *Mycobacterium smegmatis* (3) and *Nocardia farcinica* (15) confirmed that they were involved in the biosynthesis of MBT and the analog nocabactin NA, respectively, providing additional support for the idea that these gene clusters are involved the production of MBT and MBT-like siderophores.

As stated above, the megasynthase is a hybrid NRPS/PKS. These enzymes are characterized by a repeating domain architecture that recognizes and covalently tethers each precursor to the megasynthase, followed by directional condensation of the precursors to generate the nonribosomal peptide/polyketide (5). For NRPSs, the core repeating domains include an adenylation (A) domain that recognizes a particular amino or aryl acid and activates it as an acyl-AMP intermediate. These domains are viewed as the "gatekeepers" of NRPS enzymology because they control which aryl or amino acid substrates are incorporated for each position in the peptide (41, 44). The activated carbonyl of the acyl-AMP intermediate is attached to the sulfhydryl of the 4′-phosphopantetheinyl prosthetic group of the neighboring carrier protein (CP) domain, forming an acyl-*S*-CP intermediate. Condensation (C) domains then catalyze directional amide bond formation between two neighboring acyl-*S*-CPs. In some cases modified C domains, called cyclization (Cy) domains, are found in place of the C domains and form oxazolidine or thiazoline rings by catalyzing both the condensation and cyclization of Ser, Thr, or Cys residues concomitant with peptide assembly (18, 24). These domains come together to form a module (C[Cy]-A-CP), and the number of modules typically corresponds to the number of acyl or amino acids in the assembled peptide (8). For PKSs, there is an analogous set of repeating domains: (i) acyltransferase (AT) domains that recognize specific thioesterified carboxylic acids and activate them as acyl-*O*-AT intermediates, (ii) CP domains to which the precursors become tethered via thioesterification, and (iii) ketosynthase (KS) domains that catalyze the directional condensation of CP-linked precursors (19). These core domains (KS-AT-CP) form a basic PKS module analogous to a module in NRPSs. The similarities between NRPS and PKS enzymology are what enables the fusion of these systems to form NRPS/PKS hybrids.

While the genetic analysis of *mbt-1* has been fruitful, the same cannot be said for the biochemical analysis of the majority of the megasynthase components (MbtA to -F). The *in vitro* analysis has been limited to MbtA, an A domain that specifically activates salicylate, and the N-terminal CP domain of MbtB, to which the salicyl moiety is covalently tethered (29). The Cy, A, and second CP domains of MbtB were characterized as part of an artificial hybrid NRPS, confirming that these domains are able to catalyze the formation of an oxazoline or β-methyl oxazoline ring *in vitro* (6). Further analysis of the megasynthase components has been hampered by the inability to obtain soluble forms of MbtB to -F (29), which has prevented biochemical testing of their assigned functions and amino acid substrate specificity.

The *mbt-1* cluster codes for many of the enzymes needed for MBT biosynthesis, but it lacks the genes coding for the enzymes involved in the formation of the fatty acyl chain and its subsequent addition to the N^6 of the central L-Lys. A recent study identified an unlinked gene cluster (*mbt-2*) that codes for the necessary enzymes needed for this aspect of MBT biosynthesis (21). Through a series of elegant *in vitro* studies, Krithika and colleagues pieced together a potential pathway for the synthesis of the fatty acyl group, its installment on the N^6 of the central L-Lys, and hydroxylation of the N^6 of the central L-Lys and terminal caprolactam. Thus, it was proposed that the enzymes encoded by the *mbt-2* gene cluster, in conjunction the *mbt-1*-encoded MbtG, function as tailoring enzymes that modify the MBT backbone that is assembled by the NRPS/PKS megasynthase. The authors could not fully test their hypotheses biochemically because of the insolubility of most MBT megasynthase components.

Recently we (7) and others (17, 49) determined that members of the MbtH-like protein superfamily are small proteins that influence the solubility and function of associated NRPS compo-

TABLE 1 Primers used for PIPE cloning

Primer	Sequence (5′→3′)
MbtHpTEVPIPEFor	GTATTTTCAGGGCGCTAGCCATATGAGCACCAATCCTTTCGATG
MbtHpTEVPIPERev	GCTCGAGAATTCCATGGCTCAGTCCTCGACCATGGCGTCACG
pTEVPIPEFor	GCCATGGAATTCTCGAGC
pTEVPIPRev	ATGGCTAGCGCCCTGAAAATAC
MbtHpACYCNcoIPIPEFor	TTAATAAGGAGATATACCATGAGCACCAATCCTTTCGATG
MbtHpACYCHindIIIPIPERev	TTATGCGGCCGCAAGCTTTCAGTCCTCGACCATGGCGTC
pACYCNcoIPIPE	TTAATAAGGAGATATACCATG
pACYCHindIIIPIPE	TTATGCGGCCGCAAGCTT
MbtB-NdeI	CCGCGCGGCAGCCATATGGTGCATGCTACGGCGTGCTCG
MbtB-HindIII	GAGTGCGGCCGCAAGCTTTTATCGGACATCGGCACTCAC
MbtE-NdeI	CCGCGCGGCAGCCATATGTGGTTCGTGCAGATGGCCGAC
MbtE-HindIII	GAGTGCGGCCGCAAGCTTTCACGGCCACTGGTCCCATGA
MbtF-NdeI	CCGCGCGGCAGCCATATGGGACCAGTGGCCGTGACGCGA
MbtF-HindIII:	GAGTGCGGCCGCAAGCTTTCATGCTGTTATCTCCGCCAG

nents. One of the most important proposals from these studies is that NRPSs that were previously recalcitrant to *in vitro* analysis due to insolubility or inactivity issues may become soluble and active when coproduced with their cognate MbtH-like protein. This protein superfamily is named after its founding member, MbtH, a protein of unknown function in MBT biosynthesis (29). It is possible that the prior insolubility problems with the NRPS components MbtB, MbtE, and MbtF were due to heterologous production in the absence of MbtH. Therefore, coproduction of MbtH with these enzymes may provide soluble and active forms of these enzymes for *in vitro* analysis. This would allow the amino acid specificity of the A domains of MbtB, MbtE, and MbtF to be assessed. Because A domains are the "gatekeepers" of NRPSs and select for the correct substrate to be incorporated into the growing peptide, defining A domain substrate specificity establishes where that particular NRPS fits into the biosynthetic scheme and whether modifications to the amino acids seen in the final product occur before or after peptide synthesis by the NRPS. Here we show that the solubility and activity of MbtB, MbtE, and MbtF are influenced by the presence of MbtH. Furthermore, we define the A domain substrate specificities of each protein, which leads to a revision of the proposed MBT biosynthetic pathway and the possibility that additional steps in MBT biosynthesis have yet to be identified.

MATERIALS AND METHODS

Plasmid construction. The genes coding for MbtB, MbtE, MbtF, and Rv1347c in *M. tuberculosis* mc^{2}6020 were cloned into the overexpression vector pET28b (EMD Chemicals) using polymerase incomplete primer extension (PIPE)-based cloning (20). Each construct resulted in the production of a protein with an N-terminal hexahistidine tag. PIPE cloning was also used to introduce *mbtH* into the expression vectors pTEV5 and pACYC-Duet1. The pTEV5 construct produced MbtH with an N-terminal hexahistidine tag that was removable using tobacco etch virus (TEV) protease. The pACYC-Duet1 expression vector overproduced untagged MbtH. The primers used for PCR amplification are listed Table 1.

Overproduction and purification of MbtB, MbtE, MbtF, Rv1347c, and MbtH. All proteins in this study were overproduced in *Escherichia coli* BL21(DE3)ybdZ::aac(3)-IV (7). Strains overproducing MbtB, MbtE, and MbtF also contained either the pACYC-Duet1-MCS empty vector or pACYC-Duet1-MbtH, which overproduced untagged MbtH. In all cases, the overproducing strains were grown in 3 liters of LB containing the appropriate antibiotics (kanamaycin [50 μg/ml], chloramphenicol [15 μg/ml]). The cells were grown at 25°C until an optical density at 600 nm (OD_{600}) of 0.5 was reached, the temperature was shifted to 15°C, and 1 h later isopropyl-β-D-1-thiogalactopyranoside (100 μM) was added to the cultures to induce gene expression. Expression was at 15°C for 15 h. The cells were harvested by centrifugation and resuspended in buffer A (20 mM HEPES [pH 8.0], 300 mM NaCl, 10% [vol/vol] glycerol). MbtB, MbtE, MbtF, and Rv1347c purification followed previously described protocols for NRPS, and MbtH-like protein purification used nickel chelate and ion-exchange chromatography (7, 9). The protein concentrations were determined using the BCA protein assay kit (Pierce), with bovine serum albumin (BSA) as a standard.

Untagged MbtH was purified using nickel chelate chromatography before and after hexahistidine tag cleavage. Briefly, soluble protein from cell extract in buffer A supplemented with imidazole (5 mM) was batch bound to 1 ml of Ni-nitrilotriacetic acid (Ni-NTA) resin (Qiagen) at 4°C for 2 h. The resin was washed with buffer A containing 7.5 mM imidazole, and the resin was poured into a column. The proteins bound to the Ni-NTA resin were eluted using a step gradient of buffer A containing 20, 40, 60, 100, or 250 mM imidazole. Fractions containing MbtH were pooled and dialyzed overnight in buffer B (50 mM Tris-HCl [pH 8.0], 50 mM NaCl, 10% [vol/vol] glycerol) containing 0.3 mg of hexahistidine-tagged TEV protease (34). The dialyzed and TEV-digested protein was passed through 1 ml of Ni-NTA resin to remove hexahistidine-tagged MbtH and TEV protease. The untagged MbtH that did not bind to the resin was collected and concentrated. The protein concentration was determined using the BCA protein assay kit (Pierce), with BSA as a standard.

Chemical synthesis of N^6-hydroxyl-L-Lys. The synthetic scheme for N^6-hydroxy-L-Lys is shown in Fig. 2. During the synthesis procedure, ^{1}H nuclear magnetic resonance (NMR) and ^{13}C NMR were recorded on Bruker spectrometers operating at 500 and 125 MHz, respectively. Deuterated chloroform ($CDCl_3$) or perdeuterated methanol (CD_3OD) served as the solvent and internal reference. Chemical shifts are reported as ppm, and coupling constants are reported in hertz. All reagents and solvents were obtained from commercial suppliers and used without further purification. All flash chromatography was performed with normal phase silica gel (Sorbent Technologies; 32- to 63-μm particle size, 60-Å pore size), following the general protocol of Still et al. (42).

Synthesis of 2. Benzoyl peroxide (75%, 706 mg, 2.18 mmol) was added to a stirring biphasic mixture of 1 (16) (490 mg, 1.46 mmol) in buffer (7 ml, 7:3 0.75 M $NaHCO_3$–1.5 M NaOH, pH 10.5) and dichloromethane (DCM; 7 ml). After 3 h, thin-layer chromatography indicated consumption of the starting material. The reaction mixture was diluted with DCM (15 ml) and H_2O (15 ml). The layers were separated, and the aqueous portion was extracted with DCM (twice, 15 ml each). The organics were pooled, washed with 10% $Na_2S_2O_3$ (twice, 15 ml each) and brine (once, 30 ml), and then dried (Na_2SO_4), filtered, and concentrated. The

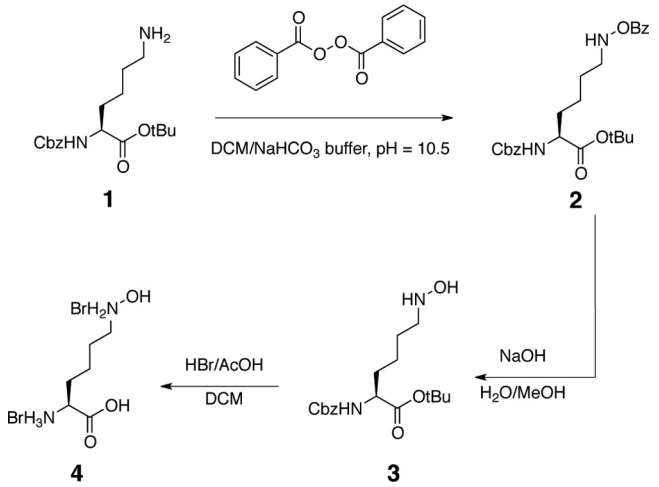

FIG 2 Schematic of the chemical synthesis of N^6-hydroxy-L-Lys. Cbz, carbobenzyloxy; tBu, *tert*-butyl; DCM, dichloromethane; Bz, benzoyl; MeOH, methanol; AcOH, acetic acid.

crude material was chromatographed on silica (1:0→9:1 DCM-ethylacetate [EtOAc]) to afford 2 as a thick syrup (512 mg, 77%).

^{1}H-NMR (500 MHz, $CDCl_3$) data were δ: 8.06 (2 H, dd, $J = 6.8$ Hz, 0.5 Hz), 7.97 (1 H, s), 7.60 (1 H, m), 7.48 (2 H, m), 7.41 to 7.31 (5 H, m), 5.73 (1 H, d, $J = 8$ Hz), 5.15 (2 H, s), 4.34 (1 H, m), 3.15 (2 H, t, $J = 6$ Hz), 1.91 (1 H, m), 1.71 (3 H, m), 1.39 (11 H, m).

^{13}C-NMR (125 MHz, $CDCl_3$) data were δ: 172.9, 167.2, 156.4, 136.9, 133.7, 129.7, 129.5, 128.9, 128.8, 128.7, 128.4, 82.3, 67.1, 55.3, 53.6, 32.2, 27.7, 26.6, 22.1.

Synthesis of 3. An aqueous solution of NaOH (1.5 M, 550 μl, 0.83 mmol) was added to a solution of 2 (250 mg, 0.55 mmol) in methanol (5 ml) under an N_2 atmosphere. After 40 min thin-layer chromatography indicated the loss of the starting material. The reaction mixture was diluted with H_2O (15 ml), which produced a white precipitate. The mixture was extracted with diethyl ether (Et_2O) (3 times, 10 ml each). The organic fractions were pooled and washed with brine (twice, 20 ml each) and then dried ($MgSO_4$), filtered, and concentrated. Filtration and concentration yielded a colorless clear oil. The crude material was purified on silica with 33:1→30:1 DCM-methanol containing 0.1% NH_3 to afford 3 (157 mg, 81%) as a cloudy oil.

^{1}H-NMR (500 MHz, $CDCl_3$) data were δ: 7.35–7.29 (5 H, m), 5.49 (1 H, d, $J = 8$ Hz), 5.10 (2 H, s), 4.26 (1 H, m), 4.12 (1 H, br s), 3.34 (1 H, br s), 2.89 (2 H, m), 1.80 (1 H, m), 1.70 to 1.50 (3 H, m), 1.45 (9 H, s), 1.42 to 1.30 (2 H, m).

^{13}C-NMR (125 MHz, $CDCl_3$) data were δ: 172.1, 156.4, 136.8, 158.9, 128.54, 128.52, 82.5, 67.3, 54.6, 53.8, 33.2, 28.4, 26.9, 23.0.

Synthesis of N^6-hydroxy-L-Lys (4). 3 (38 mg, 0.11 mmol) was dissolved in DCM (1 ml) in a vial under N_2. HBr (33% solution in acetic acid [AcOH], 1 ml) was added via syringe down the side of the vial. The resulting brown solution was stirred at room temperature (RT) for 1 h. Volatiles were removed via an N_2 stream, and the remaining liquid was removed under reduced pressure. The residue was processed in an azeotropic solution twice with PhMe and then triturated with Et_2O and DCM to afford the desired product. Spectroscopic data were as previously described (12).

Enzymatic synthesis of N^6-acyl-L-Lys and N^6-acyl-N^6-hydroxy-L-Lys. The previously reported reaction conditions for Rv1347c catalysis were used to catalyze N^6 acylation of L-Lys and N^6-hydroxy-L-Lys (11, 21). Briefly, 3.3 μg of Rv1347c was added to a 350-μl reaction mixture of 100 mM Tris-HCl, pH 8.0, 1 mM decanoyl-coenzyme A (decanoyl-CoA), and 500 μM L-Lys or N^6-hydroxy-L-Lys. Reaction mixtures containing N^6-hydroxy-L-Lys were incubated at 25°C for 3 h, while reaction mixtures containing L-Lys were incubated at 25°C for 20 h.

Enzymatic synthesis of N^6-acyl-N^6-hydroxy-L-Lys and N^6-acyl-L-Lys was monitored and quantified using a combination of 5,5′-dithiobis-(2-nitrobenzoic acid) (DTNB)- and high-pressure liquid chromatography (HPLC)-based assays. Briefly, the progression of the N^6-hydroxy-L-Lys-containing reaction was monitored using an established DTNB-based assay that monitors the release of free CoA from decanoyl-CoA after Rv1347c-dependent acylation of N^6-hydroxy-L-Lys (11, 21). The amount of N^6-acyl-N^6-hydroxy-L-Lys formed was determined using the molar extinction coefficient of 5-thio-2-nitrobenzoate (14,150 M^{-1} cm^{-1}), which is formed when free CoA reacts with DTNB (31). The amount of N^6-acyl-N^6-hydroxy-L-Lys was determined to be 31.5 nmol (90 μM final concentration) after 3 h of incubation at 25°C. This assay was not reliable for quantifying the amount of N^6-acyl-L-Lys produced because the rate of CoA release was near that for the no-amino-acid control.

An HPLC-based assay was used to quantify the amount of N^6-acyl-L-Lys produced. Briefly, 50 μl of an Rv1347c-catalyzed reaction mixture was removed and added to an equal volume of *o*-phthalaldehyde (OPA). The OPA-derivatized reaction components were separated by reverse-phase HPLC using a C_{18} column (Grace C_{18} small pore, 250 by 4.6 mm). Separation was carried out using a water-acetonitrile (MeCN) gradient containing 0.1% (vol/vol) trifluoroacetic acid and 0% MeCN for 0 to 5 min, 0 to 100% MeCN for 5 to 20 min, and 100% MeCN for 20 to 30 min. The gradient was run at a flow rate of 1 ml/min. The elution of OPA-derivatized molecules was monitored for absorbance at 340 nm, and the area under the peak associated with derivatized N^6-acyl(decanoyl)-L-Lys was quantified using Beckman-Coulter 32K software. The identity of the OPA-derivatized N^6-acyl(decanoyl)-L-Lys was confirmed by electrospray ionization mass spectrometry (ESI-MS; theoretical $m/z = 415.3$ $[M\text{-}H]^-$, observed $m/z = 415.2$ $[M\text{-}H]^-$). To quantify the amount of N^6-acyl(decanoyl)-L-Lys, known amounts of N^6-acyl(decanoyl)-N^6-hydroxy-L-Lys were derivatized with OPA and analyzed by reverse-phase HPLC and the area under the eluting peaks was quantified. These data were used estimate the amount of N^6-acyl-L-Lys that was enzymatically synthesized. The identity of the OPA-derivatized N^6-acyl-N^6-hydroxy-L-Lys was confirmed by ESI-MS (theoretical $m/z = 431.3$ $[M\text{-}H]^-$, observed $m/z = 431.2$ $[M\text{-}H]^-$). All MS was performed at the University of Wisconsin Biotechnology Center.

Amino acid-dependent ATP-PP_i exchange assays. Amino acid-dependent ATP-PP_i exchange assays were performed as previously described (7, 9). Briefly, each 100-μl reaction mixture contained 75 mM Tris-HCl (pH 7.5), 10 mM $MgCl_2$, 5 mM dithiothreitol, 3.5 mM ATP (pH 7.0), 1 mM [^{32}P]PP_i (0.9 Ci/mol), and various concentrations of amino acid and enzyme. For amino acid specificity studies all amino acids were present at 1 mM, with the exception of N^6-decanoyl-L-Lys and N^6-decanoyl-N^6-hydroxy-L-Lys, which were present at 15 μM. Enzyme concentrations used are noted in the appropriate figures. All assays were performed in the linear range for enzyme concentration, with less than 10% substrate-to-product conversion. The pseudo-first-order kinetic parameters for amino acid activation were determined by holding the ATP concentration constant at 3.5 mM while varying the amino acid concentration. For MbtB reactions the L-Thr concentrations were 0.1, 0.3, 0.6, 0.8, 1.25, 3.0, and 5.0 mM. For MbtF reactions, the amino acid concentrations were as follows: L-Lys, 25, 50, 75, 100, 150, 200, and 300 mM; N^6-hydroxy-L-Lys, 10, 25, 50, 75, 100, 200, and 300 μM. All kinetic parameters were calculated using nonlinear regression analysis (KaleidaGraph) with data from three independent assays performed in parallel.

RESULTS

MbtH influences the solubility of heterologously produced MbtB, MbtE, and MbtF. *In vitro* analysis of the MBT NRPS/PKS megasynthase has been hampered by the inability to heterologously produce soluble forms of these enzymes (29). We (7) and others (17, 49) recently determined that proteins belonging to the MbtH-like protein superfamily influence the solubility and activity of some NRPSs. The MbtH-like protein superfamily is named

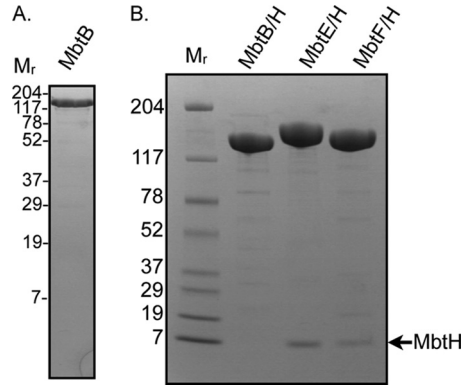

FIG 3 SDS-PAGE (4 to 20% polyacrylamide) and Coomassie staining analysis of purified NRPSs. (A) Purified MbtB (7 μg) overproduced in the absence of MbtH. (B) Purified MbtB, MbtE, and MbtF overproduced in the presence of MbtH. Eleven micrograms of protein was loaded in each lane. M_r, molecular weights (in thousands) of protein standards.

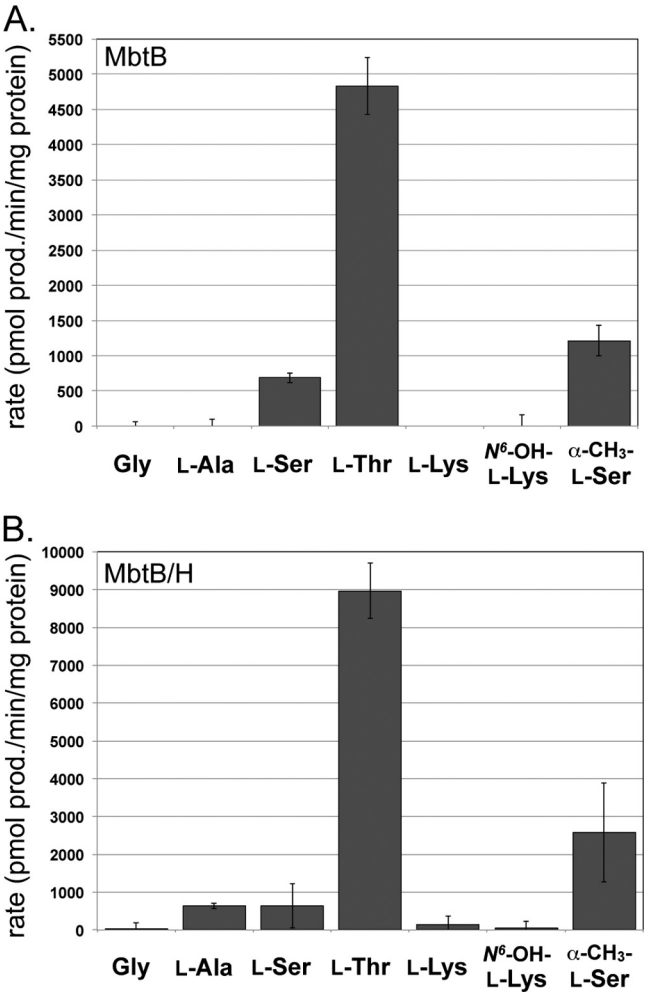

FIG 4 Amino acid specificity of the A domain of MbtB. (A) Amino acid specificity of MbtB overproduced and purified in the absence of MbtH (MbtB). (B) Amino acid specificity of MbtB overproduced and purified in the presence of MbtH (MbtB/H). The results shown are from three independent amino acid-dependent ATP/PP_i exchange reactions, with the error bars representing the standard deviations. The reaction mixtures contained either 3.8 μg (MbtB) or 4.0 μg (MbtB/H) of protein and 1 mM the noted amino acid, and the reactions were run for 20 min. A reaction mixture lacking amino acid substrate was used to define the background activation, and this activity was subtracted from that for each amino acid-containing reaction. These conditions were in the linear range of the assays for enzyme concentration, and there was less than 10% substrate-to-product conversion based on the rates of L-Ser, L-Thr, and α-methyl-L-Ser activation. Abbreviations: N^6-OH-L-Lys, N^6-hydroxy-L-Lys; α-CH_3-L-Ser, α-methyl-L-Ser.

after the founding member, MbtH, a protein of unknown function encoded by a gene in the *mbt-1* biosynthetic gene cluster. This raised the possibility that heterologous coproduction of MbtH with the NRPS components of the megasynthase (MbtB, MbtE, and MbtF) may resolve difficulties with solubility and activity of these enzymes.

MbtB, MbtE, and MbtF containing N-terminal hexahistidine tags were overproduced in *E. coli* BL21(DE3)ybdZ::aac(3)-IV (7) in the presence and absence of untagged MbtH to assess whether MbtH coproduction influenced NRPS solubility. In contrast to a prior report (29), MbtB was soluble when overproduced without MbtH (Fig. 3A); however, the presence of MbtH did influence MbtB solubility because approximately twice as much soluble MbtB was recovered from cells coproducing MbtH. MbtB overproduced in the presence or absence of MbtH was purified to near homogeneity using nickel chelate and ion-exchange chromatography (Fig. 3). MbtB did not copurify with coproduced MbtH, in contrast to other NRPSs that require MbtH-like proteins for solubility (7, 17, 49). Overproduction of MbtE or MbtF in the absence of MbtH did not result in soluble enzymes (data not shown), consistent with prior reports (29). In contrast, when MbtE and MbtF were coproduced with MbtH, both were soluble and copurified with MbtH through nickel chelate and ion-exchange chromatography (Fig. 3B). From these data we conclude that MbtH interacts with and influences the conformation of MbtB, MbtE, and MbtF, resulting in enhanced protein solubility. A mechanism for how MbtH-like proteins influence the solubility and activity of NRPSs is under investigation.

The A domain of MbtB preferentially activates L-threonine. Structural analysis of membrane-associated MBT, soluble MBT, and MBT fragments that stimulate T cell activation suggests that the oxazoline ring is formed from L-Ser, L-Thr, or α-methyl-L-Ser. These findings, when combined with bioinformatics analyses of the NRPS/PKS megasynthase enzymology, led to the proposal that the A domain of MbtB is responsible for incorporating these amino acids into MBT (4, 29). It is reasonable to hypothesize that L-Ser is the preferred substrate because the majority of the MBT purified from *M. tuberculosis* contains an oxazoline ring lacking methylation at the α or β carbon.

Standard amino acid-dependent ATP-PP_i exchange assays were used to define the amino acid specificity of the A domain of MbtB. The amino acids tested included Gly, L-Ala, L-Ser, L-Thr, α-methyl-L-Ser, L-Lys, and N^6-L-Lys. Surprisingly, the A domain of MbtB showed significant preference for L-Thr regardless of whether MbtB was overproduced in the presence or absence of MbtH (Fig. 4A and B). In fact, MbtB that was overproduced in the presence of MbtH was even more selective for L-Thr, with L-Ser activation being comparable to that observed with L-Ala (Fig. 4B). A comparison of the kinetic parameters for L-Thr activation by MbtB overproduced with or without MbtH found they were similar, with a statistically significant change observed only in the V_{max} (Table 2), which was consistent with the increased activity

TABLE 2 Kinetic parameters for amino acid activation by MbtB and MbtF[a]

Enzyme	Amino acid	K_m[b] (μM)	V_{max}[c] (pmol product/min/mg protein)	V_{max}/K_m (pmol product/min/mg protein/μM)
MbtB[d]	L-Thr	344 ± 31	11,152 ± 263	32
MbtB/H[e]	L-Thr	444 ± 53	18,025 ± 642	41
MbtB/H + MbtH[f]	L-Thr	388 ± 36	15,192 ± 528	39
MbtF/H[g]	L-Lys	40,247 ± 8,781	18,580 ± 1,126	0.46
MbtF/H	N^6-hydroxy-L-Lys	46.7 ± 4.3	210,720 ± 6,191	4,512

[a] See Fig. S1 and S2 in the supplemental material for the Michaelis-Menten plots.
[b] The values are the averages of three independent assays ± the standard errors from the nonlinear regression curve fit.
[c] The values are the averages of three independent assays ± the standard errors from the nonlinear regression curve fit.
[d] MbtB overproduced in the absence of MbtH.
[e] MbtB overproduced in the presence of MbtH.
[f] MbtB overproduced in the presence of MbtH with 100 μM MbtH added to the reaction.
[g] MbtF overproduced in the presence of MbtH.

noted in Fig. 4. Also, since MbtB did not copurify with MbtH, we tested whether the addition of MbtH to the reaction mixtures containing the MbtB coproduced with MbtH altered the kinetic parameters, but only subtle effects on both the K_m and V_{max} were observed (Table 2) and there was no change in amino acid specificity.

The A domain of MbtE is specific for N^6-acyl-N^6-hydroxy-L-lysine. The L-Lys residue adjacent to the oxazoline ring of MBT is hydroxylated and acylated at the N^6 position in the final MBT structures (Fig. 1). Prior biochemical studies suggest that N^6-acylation of the L-Lys residue occurs following its incorporation into the MBT backbone and that N^6-hydroxylation occurs subsequently (21). Based on these prior results, MbtE was predicted to activate L-Lys, and we used soluble MbtE resulting from coproduction with MbtH to test this hypothesis. Surprisingly, MbtE did not activate L-Lys. These data raised the alternate possibility that L-Lys must be modified by N^6-hydroxylation or N^6-acylation prior to activation by MbtE. Commercially available N^6-acetyl-L-Lys (to mimic N^6-acyl-L-Lys) and chemically synthesized N^6-hydroxyl-L-Lys were used in ATP-PP_i exchange assays to assess whether these modifications were required for MbtE recognition; however, neither acted as a substrate for MbtE. L-Ser, L-Thr, α-methyl-L-Ser, and α-amino-ε-caprolactam (the cyclized form of L-Lys) were also tested as substrates, but none were activated by MbtE.

Two possibilities that would explain the failure to detect MbtE activity with the substrates listed above are that N^6-acetyl-L-Lys does not have a long enough fatty acyl group for recognition by MbtE and that the true substrate for MbtE is N^6-acyl-N^6-hydroxy-L-Lys. To test these hypotheses, the previously characterized *M. tuberculosis* acyltransferase Rv1347c was used to enzymatically generate N^6-decanoyl-L-Lys and N^6-decanoyl-N^6-hydroxy-L-Lys (Fig. 5A). The decanoyl group was chosen as a mimic of the various acyl groups found on MBT, and prior work on Rv1347c showed that this enzyme efficiently recognized decanoyl-CoA as a surrogate substrate (11). The enzymatically generated substrates (at 15 μM final concentration) were used in ATP-PP_i exchange assays, and it was determined that MbtE efficiently activated N^6-decanoyl-N^6-hydroxy-L-Lys, but only weakly activated N^6-decanoyl-L-Lys (Fig. 5B).

These data strongly support a model whereby the L-Lys residue is fully modified prior to incorporation by MbtE. Furthermore, Rv1347c was determined to acylate approximately half of the N^6-hydroxy-L-Lys in a reaction mixture within 1 h, but the same amount of Rv1347c was able to acylate less than 1/10 of the L-Lys in overnight reactions. This suggests that the N^6-hydroxylation of L-Lys occurs prior to N^6-acylation. While prior analyses of Rv1347c investigated its amino acid specificity (11, 21), neither

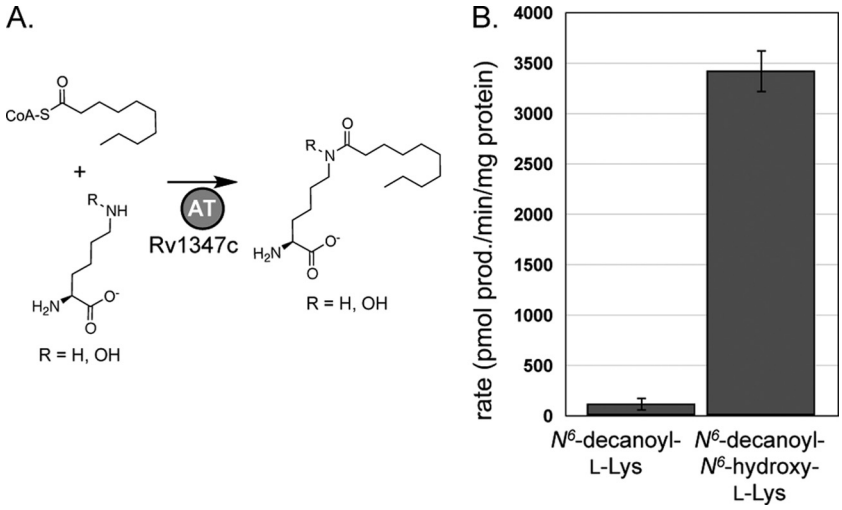

FIG 5 Amino acid specificity of the A domain of MbtE. (A) Schematic showing the substrates and products of the enzymatic synthesis of N^6-decanoyl-L-Lys and N^6-decanoyl-N^6-hydroxy-L-Lys. AT, acyltransferase. (B) Amino acid specificity of the A domain of MbtE. Results shown are from three independent amino acid-dependent ATP/PP_i exchange reactions using MbtE overproduced and purified with MbtH. The error bars represent standard deviations. The reaction mixtures contained 9 μg of MbtE/H and 15 μM each acylated amino acid, and the reactions were run for 20 min. These reaction conditions were in the linear range for enzyme concentration, and there was less than 10% substrate-to-product conversion based on N^6-decanoyl-N^6-hydroxy-L-Lys as the substrate. A reaction mixture lacking Rv1347c was used to define the background activity, and this activity was subtracted from that for each amino acid-containing reaction.

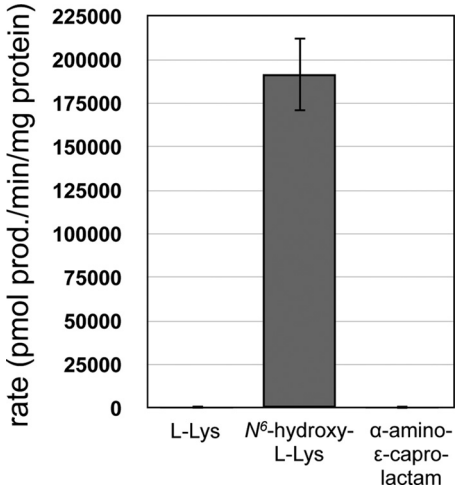

FIG 6 Amino acid specificity of the A domain of MbtF. The results shown are from three independent amino acid-dependent ATP/PP_i exchange reactions using MbtF purified with MbtH coproduction. The error bars represent standard deviations. The reaction mixtures contained 1.6 μg of MbtF/H and 1 mM each amino acid, and the reactions were run for 20 min. These reaction conditions were in the linear range for enzyme concentration, and there was less than 10% substrate-to-product conversion based on N^6-hydroxy-L-Lys as the substrate.

study tested N^6-hydroxyl-L-Lys as a substrate. Providing further support for this model are studies showing that the *M. tuberculosis* and *M. smegmatis* hydroxylase, MbtG, hydroxlyates free L-Lys (21, 33). Furthermore, MbtG homologs involved in N^5-hydroxylation of L-ornithine catalyze hydroxylation on the free amino acid prior to incorporation by the associated NRPS (25). Finally, a similar progression of N^5 acylation followed by N^5 hydroxylation of L-ornithine occurs during erythrochelin biosynthesis (32). Based on our data and these precedents, it is reasonable to conclude that L-Lys modification in MBT biosynthesis proceeds as follows: N^6-hydroxylation by MbtG, followed by N^6-acylation of N^6-hydroxy-L-Lys by Rv1347c and subsequent incorporation of N^6-acyl-N^6-hydroxy-L-Lys by MbtE.

The A domain of MbtF is specific for N^6-hydroxy-L-Lys. The finding that L-Lys must be fully modified prior to recognition by MbtE raised the possibility that MbtF would activate N^6-hydroxy-L-Lys rather than L-Lys as previously proposed. The purified MbtF/MbtH complex was assayed for amino acid activation, and a clear preference for N^6-hydroxy-L-Lys over L-Lys was observed (Fig. 6). Defining the kinetic parameters of amino acid activation revealed that the A domain showed a >10,000-fold preference (V_{max}/K_m) for N^6-hydroxy-L-Lys over L-Lys (Table 2). L-Ser, L-Thr, α-methyl-L-Ser, and α-amino-ε-caprolactam were not substrates for MbtF; thus, as seen with MbtE, the modified L-Lys is the substrate for the A domain of MbtF.

DISCUSSION

Access to soluble NRPS components of the MBT megasynthase enabled us to test hypotheses concerning the true substrates for the NRPS adenylation domains and the timing of amino acid modification during MBT assembly. Our data suggest the biosynthesis of the L-Thr-containing MBT derivatives occurs as shown in Fig. 7. First, all the necessary precursors for MBT must be biosynthesized. MbtI catalyzes the transformation of isochorismate to

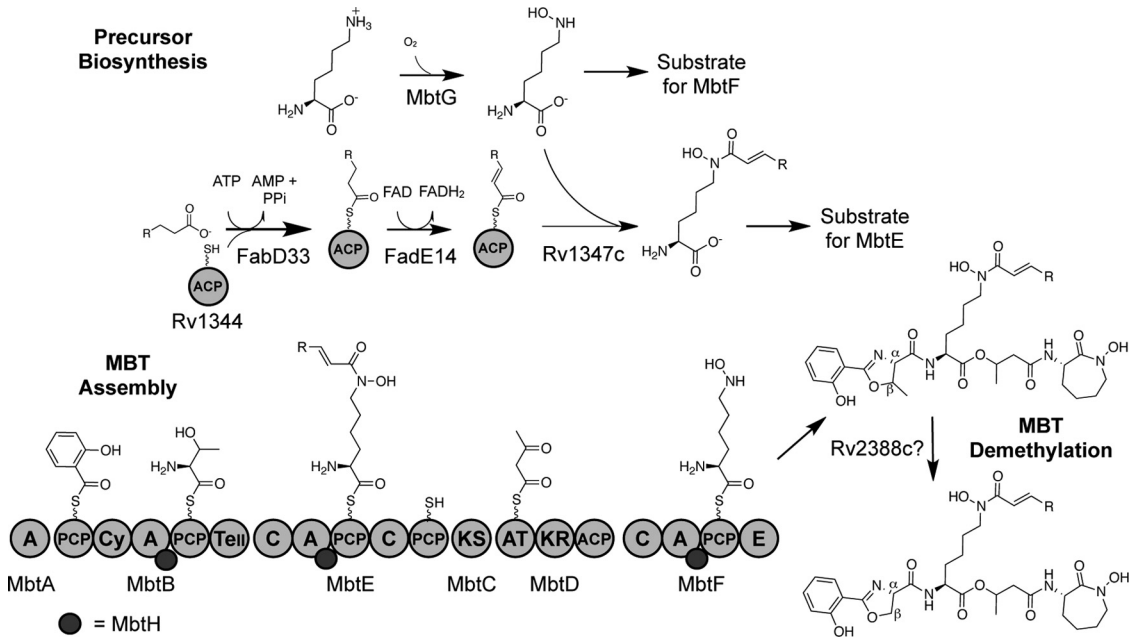

FIG 7 Proposed MBT biosynthetic pathway. For brevity, only the MBT derivatives with α,β desaturation of the fatty acyl chain are shown. Fully saturated fatty acyl chains are likely to be formed by Rv1347c recognizing substrates tethered to Rv1344 prior to FadE14 catalysis of the α,β desaturation. Enzymes previously noted as MBT tailoring enzymes are proposed to be involved in the precursor biosynthesis that provides the amino acid substrates for the NRPS components of the megasynthase. Assembly of MBT involves the function of the NRPS/PKS megasynthase, with MbtB, MbtE, and MbtF interacting with MbtH. Release of MBT from the megasynthase produces derivatives containing β-methyl oxazoline rings. The mechanism of ring demethylation is not yet known. ACP, acyl carrier protein; A, adenylation domain; PCP, peptidyl carrier protein domain; C, condensation domain; Cy, cyclization domain; TeII, type II thioesterase; KS, ketosynthase; AT, acyltransferase; KR, ketoreductase; E, epimerase.

salicylate, providing the aryl acid that caps one end of MBT (14, 29, 50). MbtG will catalyze the N^6-hydroxylation of L-Lys, generating N^6-hydroxy-L-Lys (21, 29). This is the substrate for the A domain of MbtF and also the substrate for the acyltransferase Rv1347c, which catalyzes the acylation of N^6-hydroxyl-Lys to form N^6-acyl-N^6-hydroxy-L-Lys, the substrate for the A domain of MbtE. The L-Thr substrate for the A domain of MbtB is readily available in the cell and does not have to be biosynthesized specifically for MBT assembly. Based on the final structure of MBT, it is reasonable to hypothesize that acetoacetyl-CoA is the substrate for the AT domain of the PKS portion of the megasynthase.

Once these substrates are assembled, each will be activated and thioesterified to their respective CP domains. The Cy domain of MbtB will catalyze the condensation of salicylate and L-Thr, followed by cyclization to generate the salicyl-methythiazolinyl-MbtB intermediate (6, 29). The N-terminal C domain of MbtE catalyzes the condensation of N^6-acyl-N^6-hydroxy-L-Lys-MbtE, with the upstream components tethered to MbtB. It is not clear at this point what (if any) role the additional C-CP pair at the C terminus of MbtE has in MBT biosynthesis, and further mutational analysis of MbtE is needed to determine whether these domains play any role in MBT biosynthesis. The β-keto group of the acetoacetyl moiety on MbtD will be reduced by the KR domain, generating the hydroxyl group that attacks the carbonyl of the thioesterified intermediate on MbtE, forming the ether linkage of MBT. The C domain of MbtF condenses the upstream nonribosomal peptide/polyketide hybrid molecule with the N^6-hydroxy-L-lysyl-MbtF. Cyclization of the terminal N^6-hydroxy-L-lysyl moiety, potentially by the terminal domain of MbtE, releases MBT from the megasynthase.

The described biosynthetic pathway differs from that previously proposed in the timing of the modifications to the L-Lys residues. Prior models proposed that these modifications occur after the synthesis of the backbone of MBT; thus, they are tailoring functions. Our data suggest that these enzymes are not involved in MBT tailoring; rather, they are precursor biosynthetic enzymes that generate the substrates for the NRPS components of the megasynthase. As the manuscript was being prepared, Madigan et al. published data that they interpreted as providing evidence that the hydroxylations of the L-Lys residues are the final steps in siderophore biosynthesis (23). A key piece of these data was the finding that *M. tuberculosis* still produced dideoxycarboxymycobactin (soluble MBT derivatives lacking the L-Lys hydroxylations) when *mbtG* was deleted. We interpret these data differently when we compare the relative amounts of all MBT derivatives produced in the wild-type strain versus the Δ*mbtG* strain. According to their published data, the Δ*mbtG* strain produces ≈2% of the amount of MBT derivatives that were detected in the wild-type strain, a result that is inconsistent with the model that hydroxylation is the final step in MBT biosynthesis. If hydroxylation were the final step, nearly equivalent amounts of total MBT derivatives produced in both strains would be expected, with all of the MBT in the Δ*mbtG* strain being the dideoxy derivative, while the wild-type strain would produce a distribution of the monodeoxy, dideoxy, and fully hydroxylated MBT derivatives. Taking into account our results whereby the hydroxylated substrates are the preferred substrates, we reinterpret the substantial reduction in MBT production as being consistent with our model, whereby the loss of MbtG results in the absence of the natural substrates for MbtE and MbtF. In the absence of these substrates, the structurally similar substrates L-Lys and N^6-acyl-L-Lys, respectively, are used with a lower efficiency, resulting in lower product yields. This is analogous to our findings during the analysis of viomycin biosynthesis, whereby the absence of a precursor biosynthesis enzyme resulted in the incorporation of a structurally similar, but incorrect, substrate. This change resulted in the production of a viomycin derivative at a level ≈1% of viomycin in the wild-type strain (1).

Our work provides a pathway for the biosynthesis of MBT derivatives with a β-methylated oxazoline ring but does not explain how the nonmethylated or α-methylated derivatives are generated; thus, the mechanism for removal of the β methyl group or its migration to the α carbon remains an open question. We do not favor the hypothesis that the A domain specificity of MbtB is somehow altered *in vivo* to favor L-Ser over L-Thr or α-methyl-L-Ser. Instead, we favor the hypothesis that there is a yet to be identified MBT biosynthetic enzyme(s). There is no enzyme coded within the known MBT biosynthesis gene clusters (*mbt-1* and *mbt-2*) that is a candidate for catalyzing such reactions. It is reasonable to hypothesize that a member of the radical *S*-adenosylmethionine (SAM) enzyme family is a candidate for catalyzing such demethylation or methyl group migration reactions (2, 47, 48). Interestingly, a gene (locus tag Rv2388c) encoding a class III radical SAM enzyme is upstream of *mbtI* in all *M. tuberculosis* strains as well as many other *Mycobacterium* species. Furthermore, the homolog of this gene in *M. smegmatis* (locus tag MSMEG_4525) may be in an operon with *mbtI*, raising the possibility that the encoded protein is involved in MBT biosynthesis. We note, however, that this open reading frame (ORF) is annotated as *hemN*, which codes for a radical SAM enzyme that may be involved in heme biosynthesis (22, 36); therefore, its association with MBT biosynthesis genes may be unrelated to its possible direct role in MBT assembly. Further analysis of this gene product and investigations into other potential enzyme candidates, along with labeling studies to analyze L-Thr or L-Ser incorporation into MBT, will provide additional insight into this significant question in MBT biosynthesis.

Finally, MBT biosynthesis has already proven to be a desirable target for drug development (10, 26, 45). The use of salicyl-AMP analogs initially developed by Quadri and Tan (10) and extended by others (28, 40) as inhibitors of *M. tuberculosis* growth provides a template for targeting the A domains of the MBT megasynthase for drug development. The focus on salicyl-AMP analogs to inhibit the function of MbtA was viable because these analogs were unlikely to inhibit host metabolic processes. In contrast, using L-Ser-AMP or L-Lys-AMP analogs would likely result in problematic inhibition of host tRNA synthetases. Our discovery that the A domains of MbtE and MbtF activate N^6-acyl-N^6-hydroxy-L-Lys and N^6-hydroxy-L-Lys, not L-Lys, reveals that these A domains are targets for inactivation by amino acid-AMP analogs of these nonproteinogenic amino acids. Our discovery that MbtH influences the solubility and function of MbtB, MbtE, and MbtF suggests that disrupting the interactions between MbtH and these NRPSs may provide another avenue for development of the next generation of antituberculosis drugs. We (7), and others (17, 49) have shown that eliminating MbtH-like proteins from siderophore biosynthetic pathways abolishes the ability of the associated organism to grow under iron-limiting conditions due to the disruption of siderophore biosynthesis. Importantly, MbtH is the only member of the MbtH-like protein superfamily to be encoded by *M. tuberculosis*; thus, cross-complementation by MbtH-like proteins from other NRPS systems is not an issue, as has been observed in *M.*

smegmatis (3). Finally, the described work validates the utility of MbtH-like proteins for reinvestigating medically or industrially important NRPSs that have previously proven to be recalcitrant to *in vitro* analysis.

ACKNOWLEDGMENTS

This work was funded by the NIH grant AI065850 (to M.G.T.).

We thank Adel Talaat and Sarah Marcus for the *M. tuberculosis* mc^{2}6020 chromosomal DNA. We thank Hyunjun Park for technical assistance during the analysis of MbtB.

REFERENCES

1. **Barkei JJ, Kevany BM, Felnagle EA, Thomas MG.** 2009. Investigations into viomycin biosynthesis by using heterologous production in *Streptomyces lividans*. Chembiochem **10**:366–376.
2. **Booker SJ.** 2009. Anaerobic functionalization of unactivated C-H bonds. Curr. Opin. Chem. Biol. **13**:58–73.
3. **Chavadi SS, et al.** 2011. Mutational and phylogenetic analyses of the mycobacterial *mbt* gene cluster. J. Bacteriol. **193**:5905–5913.
4. **De Voss JJ, et al.** 2000. The salicylate-derived mycobactin siderophores of *Mycobacterium tuberculosis* are essential for growth in macrophages. Proc. Natl. Acad. Sci. U. S. A. **97**:1252–1257.
5. **Du L, Sanchez C, Shen B.** 2001. Hybrid peptide-polyketide natural products: biosynthesis and prospects toward engineering novel molecules. Metab. Eng. **3**:78–95.
6. **Duerfahrt T, Eppelmann K, Muller R, Marahiel MA.** 2004. Rational design of a bimodular model system for the investigation of heterocyclization in nonribosomal peptide biosynthesis. Chem. Biol. **11**:261–271.
7. **Felnagle EA, et al.** 2011. MbtH-like proteins as integral components of bacterial nonribosomal peptide synthetases. Biochemistry **49**:8815–8817.
8. **Felnagle EA, et al.** 2008. Nonribosomal peptide synthetases involved in the production of medically relevant natural products. Mol. Pharm. **5**:191–211.
9. **Felnagle EA, Podevels AM, Barkei JJ, Thomas MG.** 2011. Mechanistically distinct nonribosomal peptide synthetases assemble the structurally related antibiotics viomycin and capreomycin. Chembiochem **12**:1859–1867.
10. **Ferreras JA, Ryu JS, Di Lello F, Tan DS, Quadri LE.** 2005. Small-molecule inhibition of siderophore biosynthesis in *Mycobacterium tuberculosis* and *Yersinia pestis*. Nat. Chem. Biol. **1**:29–32.
11. **Frankel BA, Blanchard JS.** 2008. Mechanistic analysis of *Mycobacterium tuberculosis* Rv1347c, a lysine *N*ε-acyltransferase involved in mycobactin biosynthesis. Arch. Biochem. Biophys. **477**:259–266.
12. **Genet JP, Thorimbert S, Mallart S, Kardos N.** 1993. A short route to (±)-N-hydroxylysine and (±)-laminine by palladium-catalyzed reactions. Synthesis **1993**:312–324.
13. **Gobin J, et al.** 1995. Iron acquisition by *Mycobacterium tuberculosis*: isolation and characterization of a family of iron-binding exochelins. Proc. Natl. Acad. Sci. U. S. A. **92**:5189–5193.
14. **Harrison AJ, et al.** 2006. The structure of MbtI from *Mycobacterium tuberculosis*, the first enzyme in the biosynthesis of the siderophore mycobactin, reveals it to be a salicylate synthase. J. Bacteriol. **188**:6081–6091.
15. **Hoshino Y, et al.** 2011. Identification of nocobactin NA biosynthetic gene clusters in Nocardia farcinica. J. Bacteriol. **193**:441–448.
16. **Hu J, Miller MJ.** 1997. Total synthesis of a mycobactin S, a siderophore and growth promoter of *Mycobacterium smegmatis*, and determination of its growth inhibitory activity against *Mycobacterium tuberculosis*. J. Am. Chem. Soc. **119**:3462–3468.
17. **Imker HJ, Krahn D, Clerc J, Kaiser M, Walsh CT.** 2010. N-acylation during glidobactin biosynthesis by the tridomain nonribosomal peptide synthetase module GlbF. Chem. Biol. **17**:1077–1083.
18. **Keating TA, Miller DA, Walsh CT.** 2000. Expression, purification, and characterization of HMWP2, a 229 kDa, six domain protein subunit of Yersiniabactin synthetase. Biochemistry **39**:4729–4739.
19. **Keating TA, Walsh CT.** 1999. Initiation, elongation, and termination strategies in polyketide and polypeptide antibiotic biosynthesis. Curr. Opin. Chem. Biol. **3**:598–606.
20. **Klock HE, Koesema EJ, Knuth MW, Lesley SA.** 2008. Combining the polymerase incomplete primer extension method for cloning and mutagenesis with microscreening to accelerate structural genomics efforts. Proteins **71**:982–994.
21. **Krithika R, et al.** 2006. A genetic locus required for iron acquisition in *Mycobacterium tuberculosis*. Proc. Natl. Acad. Sci. U. S. A. **103**:2069–2074.
22. **Layer G, Verfurth K, Mahlitz E, Jahn D.** 2002. Oxygen-independent coproporphyrinogen-III oxidase HemN from *Escherichia coli*. J. Biol. Chem. **277**:34136–34142.
23. **Madigan CA, et al.** 2012. Lipidomic discovery of deoxysiderophores reveals a revised mycobactin biosynthesis pathway in *Mycobacterium tuberculosis*. Proc. Natl. Acad. Sci. U. S. A. **109**:1257–1262.
24. **Marshall CG, Hillson NJ, Walsh CT.** 2002. Catalytic mapping of the vibriobactin biosynthetic enzyme VibF. Biochemistry **41**:244–250.
25. **Meneely KM, Lamb AL.** 2007. Biochemical characterization of a flavin adenine dinucleotide-dependent monooxygenase, ornithine hydroxylase from *Pseudomonas aeruginosa*, suggests a novel reaction mechanism. Biochemistry **46**:11930–11937.
26. **Monfeli RR, Beeson C.** 2007. Targeting iron acquisition by *Mycobacterium tuberculosis*. Infect. Disord. Drug Targets **7**:213–220.
27. **Moody DB, et al.** 2004. T cell activation by lipopeptide antigens. Science **303**:527–531.
28. **Neres J, et al.** 2008. Inhibition of siderophore biosynthesis in Mycobacterium tuberculosis with nucleoside bisubstrate analogues: structure-activity relationships of the nucleobase domain of 5′-O-[N-(salicyl)sulfamoyl]adenosine. J. Med. Chem. **51**:5349–5370.
29. **Quadri LE, Sello J, Keating TA, Weinreb PH, Walsh CT.** 1998. Identification of a *Mycobacterium tuberculosis* gene cluster encoding the biosynthetic enzymes for assembly of the virulence-conferring siderophore mycobactin. Chem. Biol. **5**:631–645.
30. **Ratledge C, Snow GA.** 1974. Isolation and structure of nocobactin NA, a lipid-soluble iron-binding compound from *Nocardia asteroides*. Biochem. J. **139**:407–413.
31. **Riener CK, Kada G, Gruber HJ.** 2002. Quick measurement of protein sulfhydryls with Ellman's reagent and with 4,4′-dithiodipyridine. Anal. Bioanal. Chem. **373**:266–276.
32. **Robbel L, Helmetag V, Knappe TA, Marahiel MA.** 2011. Consecutive enzymatic modification of ornithine generates the hydroxamate moieties of the siderophore erythrochelin. Biochemistry **50**:6073–6080.
33. **Robinson R, Sobrado P.** 2011. Substrate binding modulates the activity of *Mycobacterium smegmatis* G, a flavin-dependent monooxygenase involved in the biosynthesis of hydroxamate-containing siderophores. Biochemistry **50**:8489–8496.
34. **Rocco CJ, Dennison KL, Klenchin VA, Rayment I, Escalante-Semerena JC.** 2008. Construction and use of new cloning vectors for the rapid isolation of recombinant proteins from *Escherichia coli*. Plasmid **59**:231–237.
35. **Rodriguez GM, Smith I.** 2006. Identification of an ABC transporter required for iron acquisition and virulence in *Mycobacterium tuberculosis*. J. Bacteriol. **188**:424–430.
36. **Seehra JS, Jordan PM, Akhtar M.** 1983. Anaerobic and aerobic coproporphyrinogen III oxidases of *Rhodopseudomonas spheroides*. Mechanism and stereochemistry of vinyl group formation. Biochem. J. **209**:709–718.
37. **Shah NS, et al.** 2007. Worldwide emergence of extensively drug-resistant tuberculosis. Emerg. Infect. Dis. **13**:380–387.
38. **Snow GA.** 1965. Isolation and structure of mycobactin T, a growth factor from *Mycobacterium tuberculosis*. Biochem. J. **97**:166–175.
39. **Snow GA.** 1970. Mycobactins: iron-chelating growth factors from mycobacteria. Bacteriol. Rev. **34**:99–125.
40. **Somu RV, et al.** 2006. Rationally designed nucleoside antibiotics that inhibit siderophore biosynthesis of Mycobacterium tuberculosis. J. Med. Chem. **49**:31–34.
41. **Stachelhaus T, Mootz HD, Marahiel MA.** 1999. The specificity-conferring code of adenylation domains in nonribosomal peptide synthetases. Chem. Biol. **6**:493–505.
42. **Still WC, Kahn M, Mitra M.** 1978. Rapid chromatographic technique for preparative separations with moderate resolution. J. Org. Chem. **43**:2923–2925.
43. **Tsukamoto M, et al.** 1997. BE-32030 A, B, C, D and E, new antitumor substances produced by *Nocardia* sp. A32030. J. Antibiot. (Tokyo) **50**:815–821.
44. **Turgay K, Krause M, Marahiel MA.** 1992. Four homologous domains in the primary structure of GrsB are related to domains in a superfamily of adenylate-forming enzymes. Mol. Microbiol. **6**:529–546.
45. **Vasan M, et al.** 2010. Inhibitors of the salicylate synthase (MbtI) from

Mycobacterium tuberculosis discovered by high-throughput screening. Chemmedchem **5**:2079–2087.
46. **World Health Organization.** 2011. Global tuberculosis control: WHO report 2011. World Health Organization, Geneva, Switzerland. http://www.who.int/tb/publications/global_report/en/.
47. **Wu SC, Zhang Y.** 2010. Active DNA demethylation: many roads lead to Rome. Nat. Rev. Mol. Cell Biol. **11**:607–620.
48. **Zhang Q, van der Donk WA, Liu W.** 18 November 2011, posting date. Radical-mediated enzymatic methylation: a tale of two SAMS. Acc. Chem. Res. doi:10.1021/ar200202c.
49. **Zhang W, Heemstra Jr, Jr, Walsh CT, Imker HJ.** 2010. Activation of the pacidamycin PacL adenylation domain by MbtH-like proteins. Biochemistry **49**:9946–9947.
50. **Zwahlen J, Kolappan S, Zhou R, Kisker C, Tonge PJ.** 2007. Structure and mechanism of MbtI, the salicylate synthase from *Mycobacterium tuberculosis*. Biochemistry **46**:954–964.